potential. Moreover, we have noted that the general three-dimensional differential approximation is quite akin to the one-dimensional form in that the Milne-Eddington directional approximation appears to be equivalent to the replacement of an exponential integral by an exponential with a different coefficient.

References

[1] Traugott, S. C., "A differential approximation for radiative transfer with application to normal shock structure," Proc. Heat Transfer Fluid Mech. Inst. 3 (1963).

[2] Cheng, P., "Two-dimensional radiating gas flow by a moment method," AIAA J. 2, 1662–1664 (1964).

[3] Bateman, H., *Partial Differential Equations of Mathematical Physics* (Cambridge University Press, Cambridge, 1959), pp. 189 ff.

[4] Goulard, R., "Fundamental equations of radiation gas-dynamics," *The High Temperature Aspects of Hypersonic Flow*, edited by W. C. Nelson (The Macmillan Company, New York, 1964), p. 550.

[5] Traugott, S. C., "A differential approximation for radiative transfer with application to normal shock structure," The Martin Co. Research Rept. RR-34, p. 16 (December 1962).

Transition of Air Laminar Boundary Layers

D. E. Bloxsom Jr.*
Rhodes and Blossom, Canoga Park, Calif.

Nomenclature

w	=	insulated wall condition
w_1	=	insulated wall condition at end of laminar flow (start of transition to turbulent flow)
w_2	=	insulated wall condition at end of transition (fully developed turbulent flow)
∞	=	freestream conditions
s	=	conditions behind normal shock
R	=	universal gas constant
m	=	molecular weight
ρ	=	density
u	=	velocity
d	=	length of flow along body
Re	=	Reynolds number
μ	=	viscosity
Y	=	roughness length in boundary layer
θ^*	=	boundary-layer momentum thickness
$\bar{u}$	=	fluctuation in freestream velocity (magnitude of velocity disturbance)
M	=	characteristic length of freestream turbulence mechanism
d/M	=	scale parameter of freestream turbulence
$\bar{u}/u_\infty$	=	magnitude of freestream turbulence
K_H	=	Stanton number, dimensionless heat-transfer parameter
Λ	=	Karman-Pohlhausen stability parameter
C_f	=	skin-friction coefficient
P	=	pressure

Introduction

RECENT high enthalpy data indicate rapid increases of transition freestream Reynolds number with increasing enthalpy.[1–4] The boundary layer, however, under these high enthalpy conditions does not see the freestream condition, but another condition, which is much hotter and less dense than the freestream. Figure 1 shows definition of Reynolds numbers for transition.

Von Karman[5] used the insulated adiabatic wall fluid conditions to obtain a modified Reynolds number (Re_w),

Received September 21, 1964; revision received January 18, 1965.

* Partner. Member AIAA.

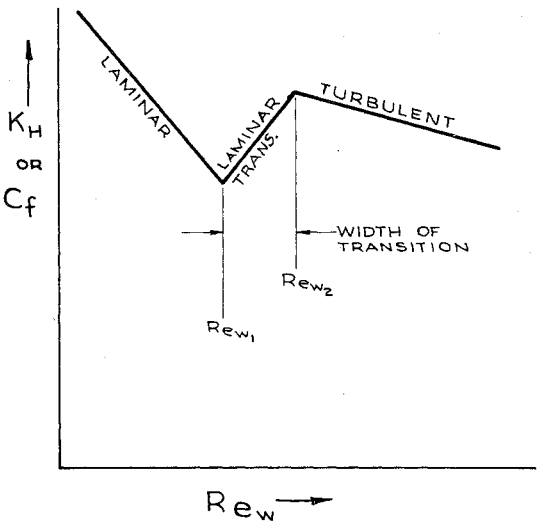

Fig. 1 Definition of Reynolds numbers.

which was then used in order to correct for compressibility effects

$$Re_\infty = \rho_\infty u_\infty d/\mu_\infty$$

is modified to

$$Re_w = \rho_u u_\infty d/\mu_w$$

By use of this early correlation, the data of Refs. 1–4, plus some incompressible data of Refs. 6–8, are correlated independent of velocity in the 450- to 16,000-fps region. This is seen in Fig. 2. A residual parameter, describing the size of freestream or roughness element at the wall relative to the boundary-layer momentum thickness, is present in data at all these velocities. The final Reynolds numbers (Re_{w_1}) for transition obtained vary from 250,000, for a roughness element of 1% of the momentum thickness, to 26,000, for a roughness element equal to the momentum thickness.

Effect of High Enthalpy

In order to transform the freestream Reynolds numbers into local modified Reynolds numbers as described previously, a series of computations was made to change the freestream conditions to conditions behind the normal shock. This was done with the Rankine-Hugoniot condition for mass-flow observation, $\rho_\infty u_\infty = \rho_s u_s$, coupled with the real gas viscosity change due to stagnation temperature rise. This latter rise of the local viscosity is the only change in the freestream Reynolds numbers under these conditions. The Reynolds number behind the normal shock is less, due to this rise in the viscosity

$$Re_s = \rho_s u_s d/\mu_s = \rho_\infty u_\infty d/\mu_s$$

A second series of computations was made to transform the freestream Reynolds numbers into equivalent modified Reynolds numbers as described previously. This series was made by the assumption that the static pressure was conserved across the boundary layer, and hence the following equation held that

$$P_\infty = P_w = \rho_\infty (R/m_\infty) T_\infty = \rho_w (R/m_w) T_w$$

These flat-plate Reynolds numbers (Re_w) are considerably less than the local Reynolds numbers behind the normal shock (Re_s), due to the additional drop of the local density. Both sets of local Reynolds numbers are plotted against velocity in Fig. 2. It will be seen for satellite conditions, 25,000 fps, that the normal-shock local Reynolds numbers are a factor of 7 below the freestream Reynolds numbers, whereas the flat-

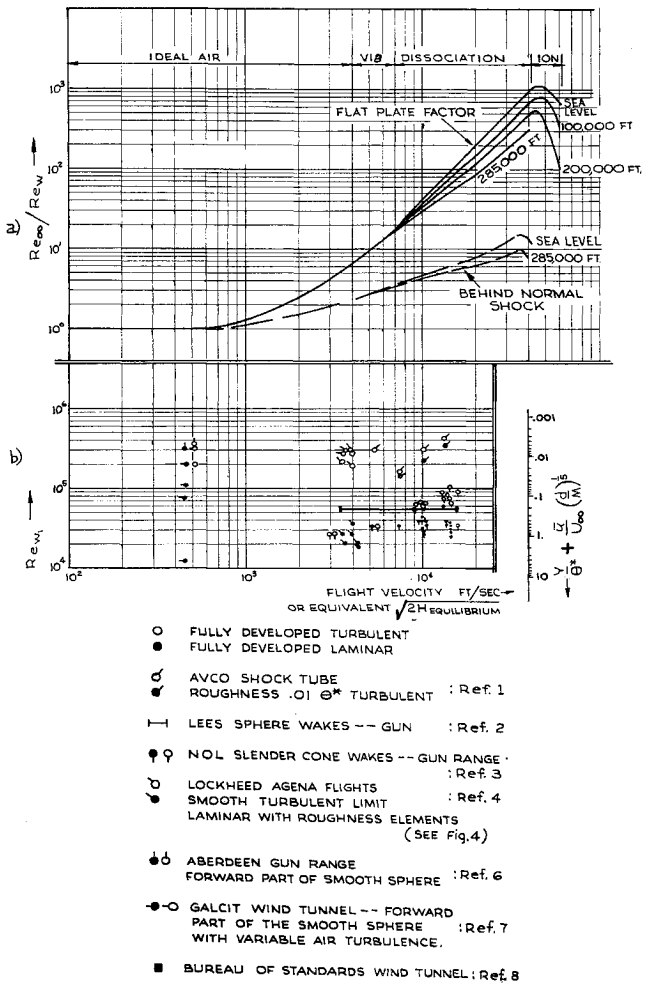

Fig. 2 a) Transformation of Re_∞ into Re_w; b) Correlation of Re_{w_1} with flight velocity.

plate local Reynolds numbers are 120 times lower than the freestream Reynolds numbers.

Effects of Freestream Turbulence and Body Roughness

Data are plotted as a function of body roughness, expressed as a ratio of momentum thickness Y/θ^* for the start of transition from laminar flow. The parameter $\bar{u}/\bar{u}_\infty(d/M)^{1/5}$ holds for freestream turbulence with the same value of transition.

Figure 3 gives experimental justification of the following equation:

$$Re_{w_1} = 26{,}000/[Y/\theta^* + \bar{u}/u_\infty(d/M)^{1/5}]^{1/2}$$

Since the data from Refs. 1, 4, and 8 are correlated to $\pm 15\%$ by means of the assumption of a constant Λ of the Karman-Pohlhausen theory of laminar boundary layers,[7] universal predictions of Re_{w_1} can be made to this accuracy.

Width of the Transition Zone

Width of the transition zone, from fully developed laminar to fully developed turbulent, is a function of Re_{w_1} as is shown in Fig. 4. Above an Re_{w_1} of 450,000, $Re_{w_1} \rightarrow Re_{w_2}$.

Validity of Testing

Since the technique correlates wind-tunnel, shock-tube, wake, and flight data, it is probably of universal validity. Since the boundary-layer transition is shown to depend on Mach number, Reynolds number, specific enthalpy, wall roughness, freestream turbulence (magnitude and scale), and geometry, these parameters must be matched in test to

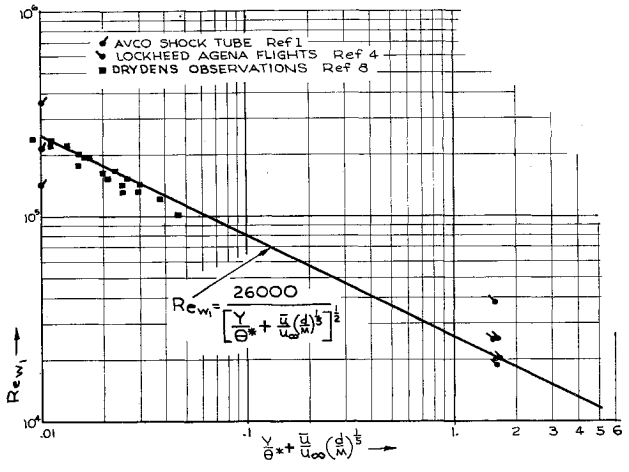

Fig. 3 Equation 5: correlation of Re_{w_1} with $Y/\theta^* + (\bar{u}/u_\infty)(d/m)1/5$.

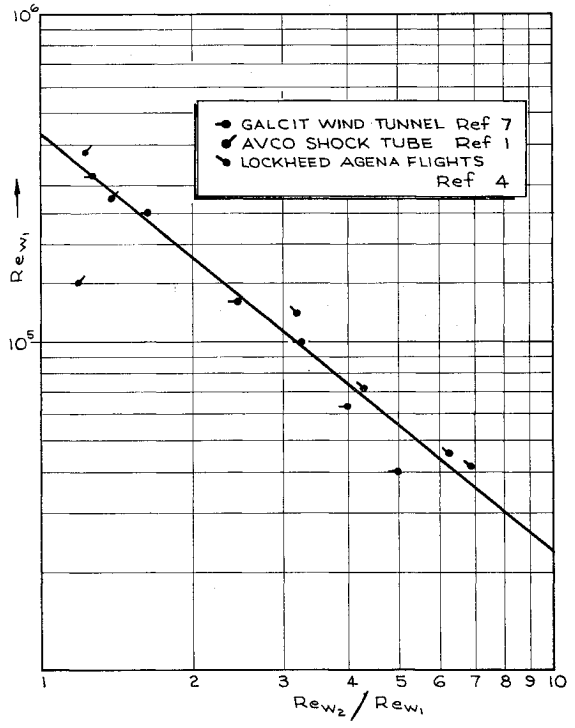

Fig. 4 Width of transition zone transformation of Re_{w_1} into Re_{w_2}.

provide valid transition data for purposes of scaling from test data to flight conditions.

Conclusions

A method is given whereby transition can be estimated to plus or minus 15% in Reynolds number at any velocity from 450 to 16,000 fps, provided potential flow and wall (or stream) roughness is known. The correlation, using Von Karman's insulated adiabatic wall Reynolds numbers, is extended to 60,000-fps velocities and altitudes from sea level to 285,000 ft. Additional computations are given for special cases of behind-normal shock and flat-plate ratios of freestream to local wall Reynolds numbers.

References

[1] Stetson, K. F., "Boundary layer transition on blunt bodies with highly cooled boundary layers," Aerospace Eng. **27**, 81 (1960).

[2] Lees, L, "Hypersonic wakes and trails," AIAA J. 2, 417–428 (1964).
[3] Lyons, W. C., Jr., Brady, J. J., and Levensteins, Z. J., "Hypersonic drag, stability, and wake data for cones and spheres," AIAA J. 2, 1948–1956 (1964).
[4] Dunn, M. G., "Effects of three-dimensional roughness elements on boundary-layer transition and aerodynamic heating," J. Spacecraft 1, 68–72 (1964).
[5] Von Karman, T., "The problem of resistance in compressible fluids," *Acts of the Fifth Convention of the Alexander Volta Foundation* (1935).
[6] Charters, A. C. and Thomas, R. N., "The aerodynamic performance of small spheres from subsonic to high supersonic velocities," J. Aeronaut. Sci. 12, 486 (1945).
[7] Goldstein, S. "Galcit Wind Tunnel Data," *Modern Developments in Fluid Dynamics* (Oxford University Press, New York, 1950), Vol. 2, p. 495.
[8] Dryden, NACA Rept. 392 (1931).

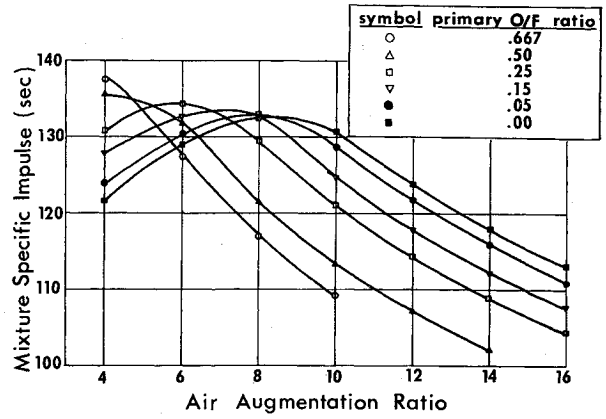

Fig. 2 Intermediate I_s vs air augmentation ratio.

Specific Impulse Calculations for Air-Breathing Propulsion

DONALD R. ALLEN* AND WILLIAM M. BYRNE JR.†
Beech Aircraft Corporation, Wichita, Kansas

Nomenclature

A = area
AA = air augmentation ratio
F = thrust
g = gravitational acceleration
Is = specific impulse
O/F = ratio of propellant oxidizer to fuel
P = pressure
V = velocity
$\dot{w}$ = weight flow rate

Subscripts

e = exit
f = fuel
j = jet
m = mixture
n = net
o = oxidizer
p = propellant
$p{\cdot}n$ = propellant net
∞ = freestream conditions

Introduction

THE rapid rise in the number of potential applications of air-breathing rocket propulsion systems to low-altitude hypersonic missions has caused the writers to develop a quick and simple method for calculating performance of propellants for these systems. This note describes a method for making air-breathing propellant performance calculations with the assistance of chemical equilibrium composition computer programs of the type normally used for rocket propellant performance calculations.

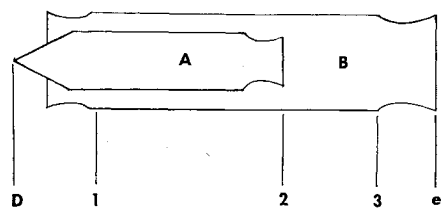

Fig. 1 Combustion apparatus model.

The theoretical model for this calculation method is shown in Fig. 1. The onboard propellants are reacted in a primary combustion chamber (A), and the resultant fuel-rich products are then exhausted into the main combustion chamber (B). In the main combustion chamber (B), the fuel-rich products are subsonically reacted with ram air and are then expanded through a supersonic nozzle to the atmosphere. The working substance in the main combustion chamber is considered to be homogeneous and invariant in composition as it passes station 3 (Fig. 1). The combustion pressure in the main chamber never exceeds the ram recovery pressure. And, for the examples used in this note, the main chamber combustion pressure was defined as being exactly equal to the maximum ram recovery pressure.

The net specific impulse for the onboard propellant under given conditions of air augmentation is readily derived from the output of the previously mentioned computer program.

Method

The chemical equilibrium composition program used for this method requires chemical descriptions of the propellant ingredients including air, a statement of the enthalpy of each of the propellant ingredients, and the relative amounts of fuels and oxidizers used. The ram air is treated as a portion of the oxidizer fraction. Air elements, such as nitrogen and oxygen, normally have zero for heats of formation, but in ramrocket and ramjet systems the rocket has done work on

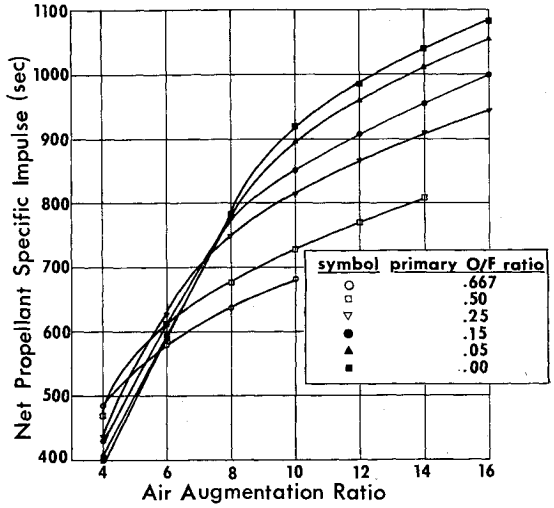

Fig. 3 Propellant I_s vs air augmentation ratio.

Received January 8, 1965.

* Technical Assistant to the Director, Missile Systems Division. Associate Fellow Member AIAA.
† Propulsion Systems Engineer, Missile Systems Division. Member AIAA.